MAGNETIC PROPERTIES OF IRON-RICH Fe–Hf GLASSES

D.H. RYAN, J.M.D. COEY

Department of Pure and Applied Physics, Trinity College, Dublin 2, Ireland

and

J.O. STRÖM-OLSEN

Physics Department, McGill University, Montreal, Canada H3A 2T8

Received 29 January 1987

Melt-spun $Fe_x Hf_{100-x}$ alloys with $x = 90$, 91 and 92 have been studied by Mössbauer spectroscopy, magnetisation measurements and low temperature specific heat. These alloys have an iron moment of $1.7\mu_B$ with an asperomagnetic spin structure. The magnetic ordering temperature falls with increasing iron content with $dT_c/dx \approx -40$ K/at%. On hydrogenation they become soft ferromagnets with $T_c \approx 300$ K and an increased iron moment of approximately $2\mu_B$. Their behaviour resembles that of amorphous iron-rich Fe–Zr.

1. Introduction

The magnetisation of iron-rich amorphous alloys $Fe_x M_{100-x}$ exhibits a variety of unusual and imperfectly understood features [1]. The magnetic ordering temperature falls on approaching the iron-rich limit in a number of cases (M = Zr [2,3], Hf [4] and B [5]) and the ground-state spin structure may lose its collinear character. While little detailed work has been reported on the magnetic properties of iron-rich a-Fe–Hf alloys, Liou et al. [6] have recently measured the [57]Fe hyperfine field and ordering temperature over the wide composition range accessible by co-evaporation ($20 \leqslant x \leqslant 94$). It is found that the ordering temperature increases to a maximum of ≈ 300 K at $x \approx 87$ then falls slightly as the iron content is raised further, whereas the hyperfine field increases monotonically with x. Here we present an account of the magnetic properties of iron-rich Fe–Hf glasses obtained by melt-spinning, and compare the results with those obtained in a parallel study of melt-spun a-Fe–Zr [3].

2. Experimental details

Alloys of the required composition were prepared by arc-melting the pure elements (purities of 3N5 or better were used) followed by melt-spinning on a copper wheel in a helium atmosphere. Ribbons 1–2 mm wide and 10 μm thick were obtained. Only a narrow range of composition could be made fully amorphous in ribbon form, $90 \leqslant x \leqslant 92$. (In the Fe–Zr system the range was twice as wide, $88 \leqslant x \leqslant 93$). X-ray diffraction on both surfaces of the samples confirmed the lack of crystallinity. Crystallisation behaviour was examined with a Perkin–Elmer differential scanning calorimeter (DSC-2) at a heating rate of 40 K/min. A single exotherm was observed at temperatures T_x listed in table 1. Samples were hydrogenated electrolytically in arsenic-doped 0.1 M K_2CO_3 solution [7]. The alloys were then quite unstable, losing their hydrogen in a matter of days at room temperature, and heating to 600 K at 25 K/min in vacuum is sufficient to drive out all the hydrogen and recover the original room-temperature proper-

Table 1

Magnetic properties of a-Fe_xH_{100-x} at 4.2 K with and without hydrogen: T_c ordering temperature, μ_z z-component of the magnetic moment, $\langle B_{hf} \rangle$ average hyperfine field, μ_0 average iron moment deduced from $\langle B_{hf} \rangle$, ψ deduced cone half-angle of the moment distribution, χ_{hf} high field slope measured at 5 T and B_c the coercivity. Also listed are crystallisation temperatures T_x and hydrogen desorption temperatures T_d with typical hydrogen contents, y

x	T_x (K)	T_c (K)	μ_z (μ_B/Fe)	$\langle B_{hf} \rangle$ (T)	μ_0 (μ_B/Fe)	ψ (°)	χ_{hf} (J/T^2kg)	B_c (mT)	T_d (K)	y
Fe_xHf_{100-x}										
90	874	233	1.62	25.9	1.73	28	0.8	5.5	–	–
91	863	182	1.54	25.7	1.71	35	1.4	12.0	–	–
92	805	155	1.48	25.7	1.71	43 or 35 [†]	2.1	43.0	–	–
$Fe_xHf_{100-x}H_y$										
90	–	≈ 300	–	30.0	2.00	0	–	–	365	10
91	–	≈ 300	2.17	30.0	2.00	0	< 0.2	< 0.3	370	8
92	–	≈ 300	2.12	30.7	2.05	0	< 0.2	< 0.2	330	13

[†] Deduced from the intensities of $\Delta m = 0$ transitions in an applied field of 2 T.

ties. Hydrogen contents and desorption characteristics were determined using a thermopiezic analyser [8] specifically constructed for hydrogen studies on milligram samples. Results are shown in fig. 1.

Magnetisation measurements were made using a vibrating-sample magnetometer in applied fields B_0 of up to 5 T provided by a superconducting solenoid. Some data were also obtained in fields of up to 9 T at the Service National de Champs Intenses in Grenoble. Ordering temperatures were determined by ac-susceptibility at a frequency of
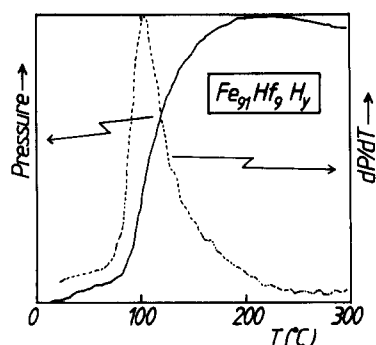

Fig. 1. Hydrogen desorption rate as a function of temperature for a-$Fe_{92}Hf_8H_{13}$ measured with the Thermopiezic Analyser at a heating rate of 20 K/min, showing pressure (solid line) and dP/dT (dotted line).

800 Hz with an rms field of 0.1 mT and also by the kink-point method in small dc fields (1–10 mT). Mössbauer spectra were obtained on a standard constant-acceleration spectrometer with a ^{57}CoRh source. A program, written by J.M. Cadogan employing the Window Fourier expansion method [9] to obtain hyperfine field distributions was used to fit the magnetically-split spectra in figs. 3, 5 and 9. A positive correlation between isomer shift and hyperfine field was included to reproduce the observed asymmetry of the spectra.

Point-by-point measurements of the low-temperature (1.5 K < T < 20 K) specific heat were obtained using a thermal relaxation method [10]; samples of order 1 mg were mounted on a 25 mm^2 diamond substrate with a metal-loaded organic adhesive.

3. Results

Magnetisation curves at 4.2 K of the three alloys studied are shown in fig. 2. Initial susceptibility is high, the magnetisation rising easily to more than 80% of its saturation value, but the final approach to saturation is very slow and a significant slope remains even in fields of 19 T. Extrapolation of data for 2 T < B_0 < 5 T to B_0 = 0 yields magnetisations which correspond to iron

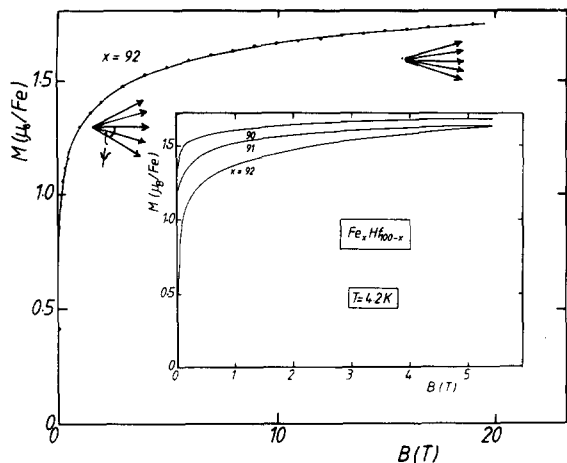Fig. 2. 4.2 K magnetisation curves for a a-Fe$_x$Hf$_{100-x}$ in fields of up to 19 T and (inset) up to 5 T. The asperomagnetic structure discussed in section 4 is illustrated.
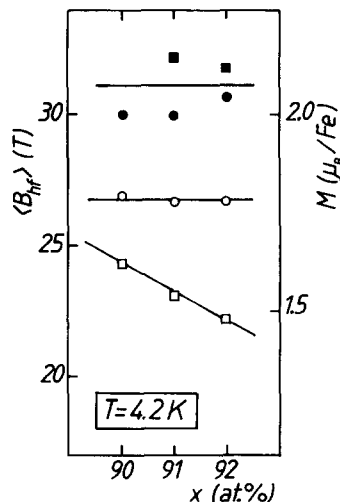

Fig. 4. Comparison of moments derived from magnetisation measurements (O) and Mössbauer spectra (□) at 4.2 K for a-Fe$_x$Hf$_{100-x}$ before (open symbols) and after (solid symbols) hydrogenation.

moments μ_z of approximately 1.5μ_B/Fe, but which fall with increasing x.

The curves in fig. 2 are similar to those obtained for other asperomagnetic systems [11], and further evidence of the noncollinear spin structure comes from Mössbauer spectra at 4.2 K (fig. 3). Those in zero applied field show a broad distribu-

tion of hyperfine fields with average values of about 25 T, corresponding to an average iron moment $\mu_0 \approx 1.7\mu_B$, which is significantly larger than that obtained by extrapolating the magnetization curves to $B_0 = 0$. (A conversion factor of 15
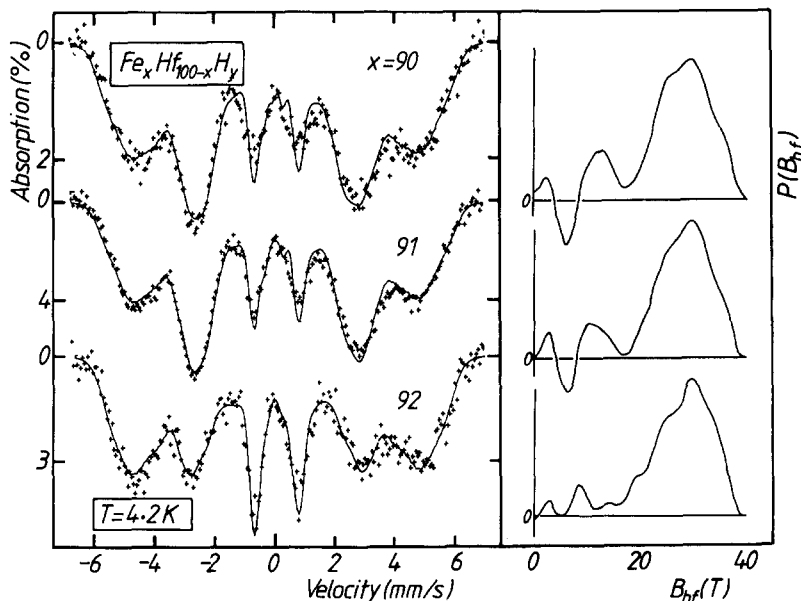

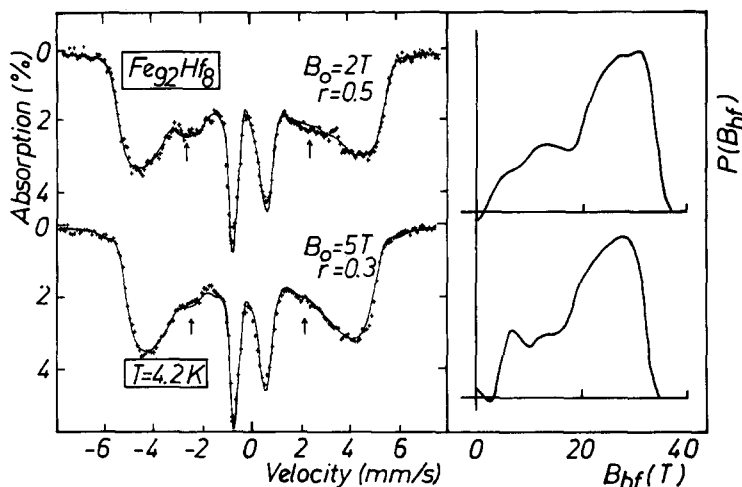Fig. 3. Mössbauer spectra of a-Fe$_x$Hf$_{100-x}$ at 4.2 K with fitted hyperfine field distributions.

Fig. 5. Mössbauer spectra of a-Fe$_{92}$Hf$_8$ at 4.2 K in external fields of 2 and 5 T, applied parallel to the γ-direction (perpendicular to the sample plane). The arrows show the positions of the $\Delta m = 0$ transitions.

T/μ_B as found in α-Fe has been used when deriving moments from Mössbauer measurements). The moments obtained at 4.2 K by Mössbauer and magnetisation measurements are compared in fig. 4.

A more direct indication of the noncollinear spin structure is provided by spectra of Fe$_{92}$Hf$_8$ in applied fields of 2 T and 5 T, as shown in fig. 5. The maximum possible value of the demagnetizing field is 1.2 T, so 2 T would be sufficient to align the ferromagnetic moment if the spin structure were collinear. Visibly this is not the case, since lines 2 and 5 (the $\Delta m = 0$ transitions) persist in

both spectra. The intensity ratio of the outer, middle and inner pairs of lines is $3 : r : 1$. The parameter r is adjusted to give the best fit, while preserving the form of the P (B_{hf}) distribution found in zero field.

The field-cooled and zero-field-cooled susceptibility in low fields is similar to that of iron-rich a-Fe$_x$Zr$_{100-x}$ [3,12]. The onset of irreversibility occurs at a temperature T_{xy}, well below T_c as indicated in fig. 6.

Low temperature specific heat of a-Fe$_{92}$Hf$_8$, plotted in fig. 7, shows the normal metallic form:
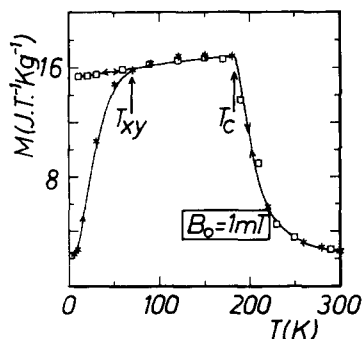
$$C = \gamma T + \beta T^3$$

Fig. 6. Susceptibility of a Fe$_{91}$Hf$_9$ in an applied field of 1 mT. Zero-field-cooled and field-cooled branches are separated below $T_{xy} \approx 50$ K.
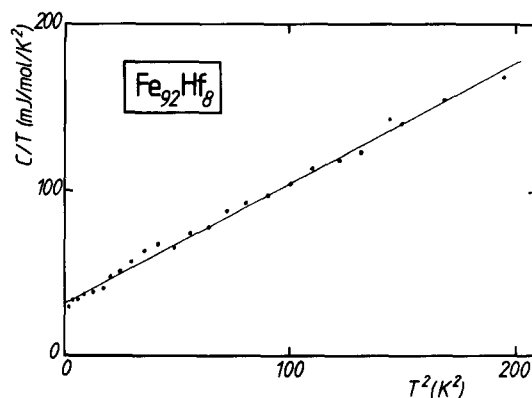

Fig. 7. Low temperature specific heat capacity for a-Fe$_{92}$Hf$_8$ plotted as C/T against T^2.
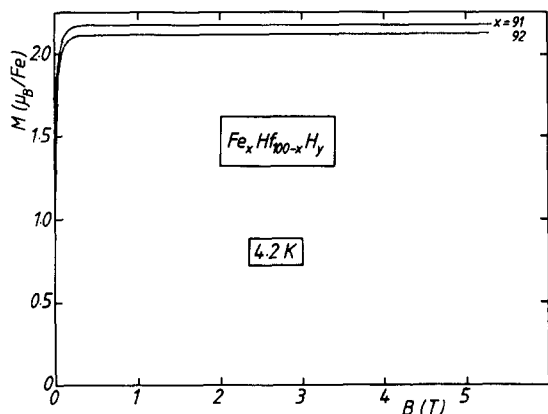
Fig. 8. 4.2 K magnetisation curves of hydrogenated a-$Fe_x Hf_{100-x}$ in fields of up to 5 T.

ture (the unstable nature of the hydrogenated alloys precludes accurate determination) and at 4.2 K they behave as good, soft ferromagnets with an increased moment and essentially zero high-field slope on the magnetisation curve (fig. 8). The hyperfine field distributions obtained from Mössbauer measurements (fig. 9) are narrower with a larger average value. Moments obtained by the two techniques are in close agreement. These results are summarised in fig. 4 and table 1.

4. Discussion

with $\gamma = 32$ mJ/mol K^2 and $\beta = 0.73$ J/mol K^4. While the coefficient of the T^3 term yields a quite reasonable Debye temperature of 140 K, the linear term is far too big to be of purely electronic origin.

The effect of hydrogen on the magnetic properties in quite dramatic. The ordering temperatures of fully-charged samples is above room tempera-

Both the persistence of the $\Delta m = 0$ absorption in large applied fields and the discrepancy at 4.2 K between the z-component of the magnetic moment (μ_z), obtained, from magnetisation measurements, and the average total moment (μ_0), obtained from Mössbauer hyperfine field distributions, point to a non-collinear spin structure. A measure of the departure from collinearity may be obtained by assuming that the moment directions, within a domain, are distributed uniformly throughout a cone of half-angle ψ about a locally-defined z-axis. Values of ψ may be ob-
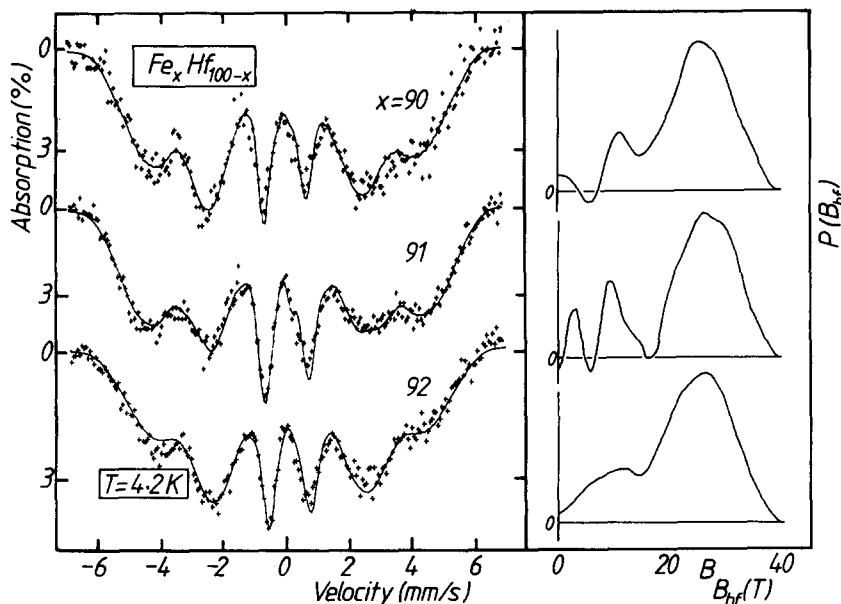

Fig. 9. Mössbauer spectra of a-$Fe_x Hf_{100-x} H_y$ at 4.2 K with fitted hyperfine field distributions.

tained from the intensities of the $\Delta m = 0$ transitions or from the ratio of μ_z to μ_0. Results in table 1 show that the degree of non-collinearity *increases* with increasing iron content. The cone picture need not be taken literally, but there exists some sort of asperomagnetic structure with a random anisotropic distribution of moment directions, and hence non-zero magnetisation within a domain. Magnetisation curves at 4.2 K (fig. 2) exhibit two distinct regions: (i) a rapid rise to $\approx 80\%$ of saturation in fields of less than 1 T, corresponding to rotation of the domains, followed by (ii) a slow approach to saturation which is incomplete, even in 19 T, as the applied field compresses the cone of moment directions.

This type of spin structure has been reported for a-Fe–Zr [3] and a-Fe–Y [13] alloys, and was attributed in both cases to a distribution of Fe–Fe exchange which includes a significant proportion of negative exchange leading to frustration of the magnetic interactions. This mixture of exchange arises because the average iron–iron separation present in these amorphous alloys lies close to the value of 0.26 nm at which the exchange interaction changes sign in fcc iron [14]. The proportion of negative exchange increases in a-Fe–Zr alloys as the fraction of iron increases; hence the strong composition and pressure-dependence of the ordering temperature in this system. The similarities between the a-Fe–Hf and a-Fe–Zr systems lead us to expect that the same mechanism is operating here, and the profound effect of hydrogenation on the magnetic properties of both systems provides further evidence of the validity of this picture. The hydrogen-induced expansion, typically 5–10% by volume for the concentrations achieved here, shifts the exchange distribution towards more positive values lifting the frustration of the order and leading to a fully collinear spin-structure. This is confirmed by the agreement between μ_z and μ_0 in the hydrogenated alloys (fig. 4).

The close similarities between iron-rich a-Fe–Hf and a-Fe–Zr extend to the irreversible susceptibility illustrated in fig. 6. The two transitions, at T_c and T_{xy}, have been analysed in some detail in the a-Fe–Zr system [3,15]. Below T_c the alloys order as wandering-axis ferromagnets with a longitudi-

nal correlation length of a few nanometers. The transverse components freeze at random only below T_{xy}, giving the asperomagnetic spin structure. Appreciable coercivity appears at still lower temperatures. Values of T_c, T_{xy}, μ_0 and μ_z are very similar for a-Fe–Hf and a-Fe–Zr alloys with the same value of x. The coercivity B_c at 4.2 K is roughly twice as large for the hafnium alloys as for their zirconium counterparts [e.g. 43 mT for a-Fe$_{92}$Hf$_8$ but 17 mT for a-Fe$_{92}$Zr$_8$), but this is not particularly significant since B_c varies exponentially with temperature.

Amorphous iron-rich Fe–Y exhibits a single spin-freezing transition at a temperature $T_f \leqslant 110$ K. The yttrium alloy with $x = 88$ behaves as one might expect the hafnium or zirconium alloys with $x \approx 95$ to behave. The differences between Hf and Zr alloys on the one hand and Y alloys on the other may be related to chemical factors. Hf and Zr have similar atomic radii (0.158 and 0.160 nm) and chemical characteristics whereas Y is larger (0.181 nm). The limited EXAFS data available on the Y [16] and Zr [17] systems suggests, however, that the average Fe–Fe distance may be 0.005 nm shorter in the Y system, which would lead to an exchange distribution containing more antiferromagnetic interactions.

The linear term in the low-temperature specific heat is far larger than that expected for a purely electronic contribution. We therefore attribute it to low-energy transverse magnetic excitations similar to those suggested for a-Fe–Zr [3]. Probably the most significant difference between the iron-rich a-Fe–Hf and a-Fe–Zr systems concerns the thermal relaxation at low temperatures. In a-Fe$_x$Zr$_{100-x}$, $x = 90$ and 92, it is found to be nonexponential on the timescale of 0.1 s, following instead a Kohlrausch law

$$T(t) = T(\infty) + \Delta T e^{-t(\tau)^{\beta'}},$$

where β' deviates from 1 below 20 K and tends to 0.5 as $T \to 0$. However, the thermal relaxation in a-Fe$_{92}$Hf$_8$ can be fitted satisfactorily to an exponential form down to the lowest temperature investigated. The difference is puzzling. There might be a connection with the greater difficulty of glass formation in the a-Fe–Hf system, re-

flected in the narrower range of x for which the samples can be prepared X-ray amorphous, If, in fact, there is some incipient microphase separation of iron in the Fe–Hf ribbons which we failed to detect by X-ray diffraction, then these iron clusters can be expected to act as magnetic relaxation centres, thereby suppressing the nonergodic behaviour.

5. Conclusion

Iron-rich amorphous Fe_xHf_{100-x} alloys order asperomagnetically below 250 K with total iron moment of $1.7\mu_B$ and a cone half-angle $\psi \approx 30°$. Hydrogenated alloys are collinear ferromagnets with increased moments and ordering temperatures above room temperature. There are very close similarities between the magnetic properties of these alloys and those of with the element above hafnium in the periodic table (zirconium) containing the same proportions of iron.

References

[1] J.M.D. Coey and D.H. Ryan, IEEE Trans. Mag. MAG-20 (1984) 1280.
[2] K.M. Unruh and C.L. Chien, J. Magn. Magn. Mat. 31–34 (1983) 1587.
[3] D.H. Ryan, J.M.D. Coey, E. Batalla, Z. Altounian and J.O. Ström-Olsen, Phys. Rev. B (to be published).
[4] T. Masumoto, S. Ohnuma, K. Shirakawa, M. Nose and K. Kobayashi, J. de Phys. 41 (1980) C8-686.
[5] C.L. Chien and K.M. Unruh, Phys. Rev. B24 (1981) 1556.
[6] S.H. Liou, G. Xiao, J.N. Taylor and C.L. Chien, J. Appl. Phys. 57 (1985) 3536.
[7] J.M.D. Coey, D.H. Ryan and Yu Boliang, J. Appl. Phys. 55 (1984) 1800.
[8] D.H. Ryan and J.M.D. Coey, J. Phys. E19 (1986) 693.
[9] B. Window, J. Phys. E4 (1971) 401.
[10] R. Bachmann, F.J. DiSalvo Jr., T.H. Geballe, R.L. Greene, R.E. Howard, C.N. King, H.C. Kirsch, K.N. Lee, R.E. Schwall, H-U. Thomas and R.B. Zubeck, Rev. Sci. Instr. 43 (1972) 205.
[11] K. Moorjani, and J.M.D. Coey, Magnetic Glasses (Elsevier, Amsterdam, 1984).
[12] H. Hiroyoshi and K. Fukamichi, Phys. Lett. A 85 (1981) 242; J. Appl. Phys. 53 (1982) 2226.
[13] J. Chappert, J.M.D. Coey, A. Liénard and J.P. Rebouillat, J. Phys. F11 (1981) 2727.
[14] W. Kummerle and U. Gradmann, Solid State Commun. 24 (1977) 33.
[15] J.M.D. Coey, D.H. Ryan and R. Buder, Phys. Rev. Lett. 58 (1987) 385.
[16] D.W. Forrester, N.C. Koon, J.H. Schelleng and J.J. Rhyne, Solid State Commun. 30 (1979) 177.
[17] Y. Waseda and H.S. Chien, in: Rapidly Quenched Metals III, vol. 1 (The Metals Society, London, 1978) p. 415.
H. Maeda, H. Terauchi, N. Kamijo, M. Hida and K. Osamura, in: Proc. 4th Intern. Conf. on Rapidly Quenched Metals (Metals Society of Japan, Sendai, 1982) p. 397.